Catalytic Ring-Opening Polymerization of Propylene Oxide by Organoborane and Aluminum Lewis Acids

Debashis Chakraborty, Antonio Rodriguez, and Eugene Y.-X. Chen*

Department of Chemistry, Colorado State University, Fort Collins, Colorado 80523-1872

Received January 15, 2003; Revised Manuscript Received May 13, 2003

ABSTRACT: Catalytic ring-opening polymerization of propylene oxide (PO) was studied with 12 organoborane and aluminum catalysts in combination with 12 hydroxylic initiators. These catalysts vary in Lewis acidity and ligand steric bulk, whereas the initiators differ in their functional groups and Brønsted acidity. This study examined four aspects of PO polymerization: degree of polymerization control, effects of catalyst and initiator structure on activity and polymer molecular weight, reactions of catalyst with initiator and catalyst with monomer, and structures of PPOs produced. In the absence of hydroxylic initiators, $B(C_6F_5)_3$ predominantly catalyzes isomerization of PO to propionaldehyde in hexanes and additionally produces low oligomers in toluene; interestingly, the sterically encumbered perfluorobiphenyl borane $B(C_{12}F_9)_3$ affords no such isomerization products. With addition of sufficient high concentration of hydroxylic initiators in a $[PO]_0$:$[-OH]_0$ ratio of 41.7, however, PPOs with the desired M_n range of a few thousand dalton and low PDI of <1.3 can be produced with the $B(C_6F_5)_3$/initiator system. The linear dependence of PPO M_n on monomer conversion is observed up to ~84% conversion. The PO polymerization activity strongly depends on Lewis acidity of the borane catalyst, with $B(C_6F_5)_3$ being most active; as Lewis acidity of the boranes decreases, the activity declines sharply. The activity is also proportional to Brønsted acidity of hydroxylic initiators, with aromatic carboxylic acids being most effective. However, excess of carboxylic acid and water initiators decomposes the borane catalyst via elimination of pentafluorobenzene, resulting in low catalytic activity and producing low oligomers; such a decomposed catalyst structure has been characterized by X-ray diffraction analysis. On the other hand, the borane catalyst is very stable toward alcohol initiators; strong activation of 1,4-butanediol, a weak Brønsted acid, by $B(C_6F_5)_3$, is demonstrated by the spectroscopic data and X-ray structural characterization for the borane:diol adducts. In comparison, the Al complexes are much less effective for PO polymerization, especially when used with hydroxylic initiators, due to the instability toward hydroxylic initiators. Nevertheless, in the absence of such initiators, alumoxane substantially free of trialkylaluminum and a three-coordinate cationic aluminum complex produce PPOs of $M_n = 4040$ and $M_n = 10\,600$, respectively. Analyses using ^{13}C NMR spectroscopy indicate that the PPOs produced from this study are atactic and essentially regioirregular, while MALDI−TOF MS spectra reveal the presence of two types of linear PPO structures having the initiator and water molecules as end groups, respectively, plus a small amount of cyclic PPO. Except for diol and triol initiators ($B(C_6F_5)_3$ as catalyst) which produce PPOs having higher primary hydroxyl contents with a typical [primary OH]/[secondary OH] ratio ≥ 60/40, the remaining PPO samples give about an equal amount of primary and secondary hydroxyl groups.

Introduction

Poly(propylene oxide) (PPO),[1] an important member of the polyether polyol family, is useful in a number of applications as key compositions for lubricants, detergents, printing inks, surfactants, cosmetic agents, and foam control agents. In particular, low to medium molecular weight PPOs of a few thousand daulton are key intermediates in polyurethane production[2] in which primary-hydroxyl-terminated polyols undergo polycondensation reactions with diisocyanates in certain rapid processes such as polyurethane reaction injection molding (eq 1). The physical and mechanical properties of polyurethanes can be modulated from rigid foams and plastics to flexible foams and elastomers, usually accomplished by controlling the chain length of the incorporated polyol and the degree of branching or crosslinking.

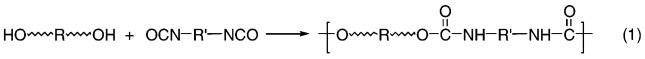

Three mechanistically distinct chemical processes are commonly used for production of PPOs through ring-opening polymerization (ROP) of propylene oxide (PO): base catalysis, acid catalysis, and coordination catalysis. Most PPOs used commercially for urethanes and surfactants are produced through a base-catalyzed, anionic ROP process, whereby PO is combined with a hydroxylic initiator and a strongly basic catalyst (e.g., potassium hydroxide).[1] The initiator compound determines the functionality of PPO (i.e., number of hydroxyl groups/molecule of product) and may also introduce some desired functional groups into the product. In the conventional KOH-initiated anionic route, ethylene oxide is often added in a subsequent step at the end of the polymerization of PO to afford the reactive, primary-hydroxyl-terminated PPOs. There are some other disadvantages of polymerizing PO using these strongly basic catalysts; for example, the basic catalyst typically must be removed from the polyol product before it is combined with the diisocyanates, which increases manufacturing costs. In addition, KOH promotes the formation of allyl alcohol that leads to a terminally unsaturated, monofunctional polyol.[3]

PO can be readily oligomerized cationically by acidic catalysts, typically Lewis acids such as boron trifluoride diethyl etherate and Brønsted acids such as HBF_4.[1,4] However, these catalysts tend to promote the formation of considerable amounts of byproducts, including dimethyldioxane and various concurrent cyclic oligomers[5]

* Corresponding author. E-mail: eychen@lamar.colostate.edu.

10.1021/ma034050a CCC: $25.00
Published on Web 06/24/2003

via "backbiting" reactions where the growing polymer chain reacts with itself. Consequently, acid catalysis is not favored industrially, despite its typically high reaction rates. To substantially reduce formation of such byproducts, Penczek and co-workers[6] have developed cationic "activated monomer" ring-opening polymerization where a heterocyclic monomer is activated via protonation by Brønsted acids such as HBF_4 and the growing chain end is the neutrally charged hydroxyl group, instead of the highly reactive, electrophilic oxonium ion (i.e., active-chain end). To suppress the reactions proceeding with the active-chain end mechanism, the "activated monomer" ROP is typically carried out under monomer starving conditions (i.e., slow addition of monomer to the catalyst/initiator mixture over a 24-h period for achieving low instantaneous concentration of monomer).

The third type of the polymerization process for ROP of PO is coordination catalysis.[7] Since the first report on the coordination polymerization of PO with ferric chloride/PO catalyst by Pruitt and Baggett[8] in 1955, various types of catalysts effective for this type of polymerization have emerged. Particularly noteworthy is the discrete (porphyrin)Al−X (X = Cl, OR, SR) initiator, developed by Inoue et al.,[9] for living or immortal coordination polymerization of PO. Spassky and co-workers[10] have used the related (Salen)Al−X coordination catalysts for PO polymerization. Chisholm and co-workers[11] have carried out mechanistic studies on coordination polymerization of PO using bulky bisphenoxide aluminum chloride dimers and compared the PO polymerization characteristics using various types of coordination catalysts. Vandenberg[12] and others[13] have used nondiscrete oligomeric alumoxanes, the product of the partial hydrolysis of trialkylaluminum, as coordination catalysts for ROP of PO and other epoxides. Lenz and Barron et al.[14] have reported stereoregular polymerization of racemic PO using isobutylalumoxane/PO complex. Generally speaking, coordination catalysts produce high polymers; such products are too high in molecular weight to be of value for polyurethane production.

The research toward ROP of PO in both academia and industry continues to focus on the development of new catalysts and more efficient and controllable catalytic polymerization systems. Double metal cyanide (DMC) catalysts are continuously paid considerable attention,[15] mostly in the patent literature. The utility of cationic aluminum complexes having various coordination numbers at aluminum (3−6) in ROP of PO has been recently explored by a number of groups. Atwood et al.[16] have used cationic aluminum complexes supported by tetradentate Salen ligands as well as boron cations supported by tridentate *O,N,O*-ligands for cationic polymerization of PO. Baugh and co-workers[17] have studied polymerization of PO with both neutral and cationic aluminum complexes incorporating various multidentate N- and O-donor ligands. Jordan et al. have briefly mentioned[18] polymerization of PO with three-coordinate alkyl aluminum cations supported by aminotroponiminate ligands, whereas Bertrand et al.[19] have used four-coordinate aluminum cations incorporating tridentate nitrogen donors for polymerization of PO. Braune and Okuda[20] have recently reported the controlled PO polymerization using a catalyst/initiator pair consisting of a neutral aluminum Lewis acid and an anionic aluminate complex.

Scheme 1[a]

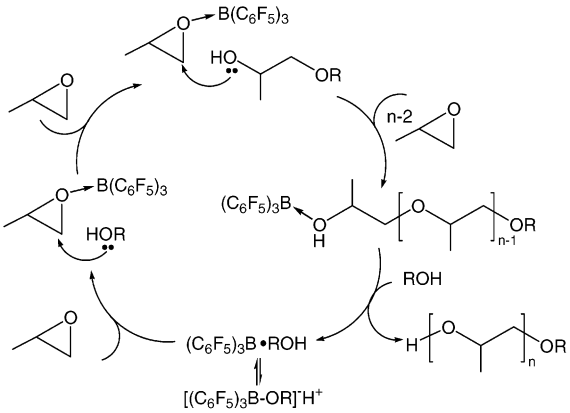

[a] A similar cycle catalyzed by H^+ and regio-isomers not shown for clarity.

Scheme 2

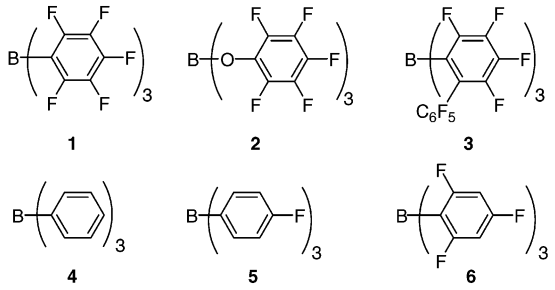

Scheme 3

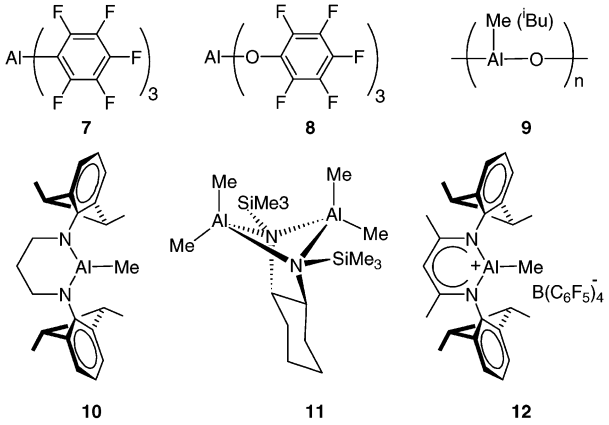

We are interested in developing a Lewis acid-catalyzed polymerization system (Scheme 1) that enables production of PPOs with the desired molecular weight range of a few thousand Da and with high catalytic activity. Herein, we report the studies of catalytic ROP of PO catalyzed by a series of organoboron (**1**−**6**, Scheme 2) and aluminum (**7**−**12**, Scheme 3) Lewis acids and initiated by 12 mono- to multifunctional hydroxylic initiators with the number of active hydrogens per molecule $f = 1, 2, 3, 8$.

Experimental Section

Materials and Methods. All syntheses and manipulations of air- and moisture-sensitive materials were carried out in flamed Schlenk-type glassware on a dual-manifold Schlenk line, on a high vacuum line, or in an argon-filled glovebox. NMR scale reactions were conducted in Teflon-valve-sealed sample J. Young tubes. Anhydrous or HPLC-grade organic solvents were first saturated with nitrogen and then dried by passage through activated alumina and Q-5 catalyst in stain-

less steel columns prior to use. Benzene-d_6 and toluene-d_8 were dried over Na/K alloy and distilled and/or filtered prior to use, whereas C_6D_5Br and $CDCl_3$ was dried over activated Davison 4 Å molecular sieves. NMR spectra were recorded on either a Varian Inova 300 (FT 300 MHz, ^{1}H; 75 MHz, ^{13}C; 282 MHz, ^{19}F) or a Varian Inova 400 spectrometer. Chemical shifts for ^{1}H and ^{13}C spectra were referenced to internal solvent resonances and are reported as parts per million relative to tetramethylsilane. ^{19}F NMR spectra were referenced to an external $CFCl_3$ standard.

Propylene oxide, anhydrous methanol, trifluoroacetic acid, benzyl alcohol, pentafluorophenol, benzoic acid, 2,4,6-trifluorobenzoic acid, 1,4-butanediol, 2,5-hexanediol, terephthalic acid, glycerin, sucrose, *n*-BuLi, 4-fluorophenylmagnesium bromide, BCl_3, BF_3·OMe_2, $AlMe_3$, chlorotrimethylsilane, (±)-*trans*-1,2-diaminocyclohexane, triethylamine, 2,6-diisopropylaniline, TMEDA, 1,3-dibromopropane, pentafluorobromobenzene, and 2,4,6-trifluorobromobenzene were purchased from Aldrich Chemical Co. and used as received unless otherwise indicated. PO, 1,4-butanediol, and 2,5-hexanediol were first degassed and dried over CaH_2 overnight and then vacuum-distilled before use.

Tris(perfluorophenyl)borane, $B(C_6F_5)_3$ (**1**), was obtained as a research gift from Boulder Scientific Co. and further purified by recrystallization from hexanes at −35 °C for polymerization studies. Triphenylborane (**4**) was purchased from Aldrich Chemical Co. and used as received. $Ph_3CB(C_6F_5)_4$,[21] tris(pentafluorophenoxy)borane (**2**),[22] perfluorobiphenyl borane (PBB, **3**),[23] and tris(4-fluorophenyl)borane (**5**)[22] were prepared according to the corresponding literature procedures.

Tris(pentafluorophenyl)alane, $Al(C_6F_5)_3$ (**7**), as a 0.5·toluene adduct, was prepared according to the literature procedure,[24] which is the modified synthesis of the alane first disclosed by Biagini et al.[25] *Caution! Extra caution should be exercised when handling this material, due to its thermal and shock sensitivity*. Tris(pentafluorophenoxy)aluminum (**8**)[26] was synthesized according to the literature procedure. Triisobutylaluminum-modified methylalumoxanes MMAO (**9**) was purchased from Azko-Nobel, whereas PMAO of substantially free of trialkylaluminum content was prepared according to the literature.[27] Aluminum complexes incorporating chelating [N⁀N] ligands, **10**,[28] **11**,[29] and **12**,[30] were synthesized according to the literature procedures.

Preparation of Tris(2,4,6-trifluorophenyl)borane (6). Borane **6** was synthesized with a procedure analogous to that for **1**.[31] To a stirred solution of 2,4,6-trifluorobromobenzene (4.47 g, 21.2 mmol) in 150 mL of hexanes at −78 °C was added *n*-BuLi (13.3 mL, 1.6 M in hexanes, 21.2 mmol). The resulting suspension was stirred at this temperature for 2 h. To this mixture, BCl_3 (7.07 mL, 1.0 M in hexanes, 7.07 mmol) was added rapidly via syringe. After being stirred at −78 °C for 30 min, the reaction mixture was gradually warmed to ambient temperature and stirred overnight. The resulting suspension was filtered to give a yellow filtrate, the solvent of which was removed under reduced pressure to produce 2.1 g (73%) of the crude product as a viscous oil. This oil was redissolved in a minimal amount of hexanes and stored at −30 °C overnight to yield crystals. These crystals were filtered, washed with 2 × 1 mL cold hexanes, and dried to give 0.75 g (26%) of the title compound. ^{1}H NMR (C_6D_6, 23 °C): δ 6.11 (t, J_{H-F} = 7.8 Hz, 6H, Ar). ^{19}F NMR (C_6D_6, 23 °C): δ −96.59 (t, J = 9.9 Hz, 6F, *o*-F), −100.26 (pent, J = 9.0 Hz, 3F, *p*-F).

Isomerization of Propylene Oxide and Isolation of CH_3CH_2CHO·$B(C_6F_5)_3$. To a stirred suspension of $B(C_6F_5)_3$ (0.20 g, 0.39 mmol) in 5 mL of hexanes at −78 °C was added a solution of propylene oxide (0.39 mmol) in 0.5 mL of hexanes. After being stirred at −78 °C for 10 min, the dry ice−acetone bath was removed and the mixture was stirred for another 30 min. The resulting suspension was filtered to give a yellow solid, which was washed with 2 × 2 mL of cold hexanes and dried, producing 0.072 g (42%) of CH_3CH_2CHO·$B(C_6F_5)_3$ as a powdery white solid. The reaction of the borane with 2 equiv of PO under the same conditions produced the same product, the propionaldehyde−borane adduct. The same reactions, when carried out in toluene, produced a mixture of many products including the propionaldehyde−borane adduct and oligomeric PPO. The reactions in hexanes were repeated using adducts $(C_6F_5)_3B$·HOMe and $(C_6F_5)_3B$·2HOMe; formation of the propionaldehyde−borane adduct was substantially suppressed in the case of $(C_6F_5)_3B$·HOMe, and only a trace amount of the propionaldehyde−borane adduct was detected for the reaction using $(C_6F_5)_3B$·2HOMe.

Spectroscopic Data for CH_3CH_2CHO·$B(C_6F_5)_3$. ^{1}H NMR (C_6D_6, 23 °C): δ 8.17 (s, 1H, C*H*O), 1.58 (q, J = 6.9 Hz, 2H, CH_2), 0.46 (t, J = 6.9 Hz, 3H, CH_3). ^{19}F NMR (C_6D_6, 23 °C): δ −134.23 (dd, J = 16.6 Hz, 6F, *o*-F), −153.87 (t, J = 19.7 Hz, 3F, *p*-F), −162.66 (tt, 6F, *m*-F). ^{13}C NMR (C_6D_6, 23 °C): δ 221.35 (*C*HO), 150.22, 147.09, 139.34, 117.36 (C_6F_5), 37.15 (CH_2), 5.72 (CH_3).

Reaction of $B(C_6F_5)_3$ with 1,4-Butanediol. To a stirred suspension of $B(C_6F_5)_3$ (0.15 g, 0.30 mmol) in 5 mL of hexanes at −30 °C was added a solution of 1,4-butanediol (0.081 mL, 0.90 mmol) in 0.5 mL of hexanes. The mixture was left stirring for 30 min after the cold bath was removed, and filtered to give a powdery white solid. The crude product was washed with 2 × 2 mL of cold hexanes and dried, producing 0.092 g (44%) of the 1:2 borane/diol adduct $HO(CH_2)_4OH$·$OH(CH_2)_4$-HO·$B(C_6F_5)_3$ (**13**). This solid was redissolved in a minimal amount of toluene and stored at −30 °C overnight to yield colorless crystals. These crystals were filtered, washed with 2 × 1 mL of cold hexanes, and dried. The NMR spectra of the adduct reveal two types of 1,4-butanediol molecules in a 1:1 ratio, indicating the formation of the 1:2 borane/diol adduct.

Spectroscopic Data for $HO(CH_2)_4OH$·$OH(CH_2)_4HO$·$B(C_6F_5)_3$ (13). ^{1}H NMR (C_6D_6, 23 °C): δ 2.97 (t, J = 4.5 Hz, 4H, CH_2OH, outer diol), 2.55 (t, J = 4.8 Hz, 4H, CH_2OH, inner diol), 1.03 (m, 4H, CH_2CH_2OH, outer diol), 0.66 (m, 4H, CH_2-CH_2OH, inner diol). ^{19}F NMR (C_6D_6, 23 °C): δ −134.21 (d, J = 20.9 Hz, 6F, *o*-F), −156.23 (t, J = 19.7 Hz, 3F, *p*-F), −163.54 (tt, 6F, *m*-F). ^{13}C NMR (C_6D_6, 23 °C): δ 150.22, 147.09, 139.34 (C_6F_5, C_{ipso} obscured), 68.66, 63.37, 29.55, 27.82 (CH_2).

Another Reaction of $B(C_6F_5)_3$ with 1,4-Butanediol. In a separate experiment, 1,4-butanediol was added to a suspension of $B(C_6F_5)_3$ in hexanes in a 1:2 molar ratio and the reaction was carried out in the same manner as for the isolation of **13**. The ^{1}H NMR spectrum of the product reveals two types of 1,4-butanediol molecules in a 1:2 ratio, indicating the formation of the 1:3 borane/diol adduct $2HO(CH_2)_4OH$·$OH(CH_2)_4HO$·$B(C_6F_5)_3$ (**14**). Single crystals suitable for X-ray diffraction study were grown from toluene at −30 °C inside a glovebox. ^{1}H NMR (C_6D_6, 23 °C): δ 3.07 (t, J = 3.9 Hz, 8H, CH_2OH, outer diol), 2.90 (t, J = 5.1 Hz, 4H, CH_2OH, inner diol), 1.15 (m, 8H, CH_2CH_2OH, outer diol), 0.87 (pent, J = 5.1 Hz, 4H, CH_2CH_2OH, inner diol). ^{19}F NMR (C_6D_6, 23 °C): δ −134.22 (d, J = 8.5 Hz, 6F, *o*-F), −156.96 (t, J = 21.2 Hz, 3F, *p*-F), −163.91 (tt, 6F, *m*-F).

Reaction of $B(C_6F_5)_3$ by 2,4,6-$F_3C_6H_2COOH$ and Isolation of $\{(C_6F_5)_2B[OC(=O)(C_6H_2F_3)]\}_2$ (15). In a glovebox, to a stirred solution of $B(C_6F_5)_3$ (0.15 g, 0.28 mmol) in 5 mL of toluene at −30 °C was added 2,4,6-$F_3C_6H_2COOH$ (0.05 g, 0.28 mmol) as a solid. After being stirred at this temperature for 45 min, NMR analysis of an aliquot indicated a composition consisting of approximately 28% for the carboxylic acid−borane adduct [2,4,6-$F_3C_6H_2C(=O)OH$·$B(C_6F_5)_3$] and 72% for the dimer product **15**. The reaction mixture was stirred for another 15 h, at which time the NMR analysis still showed the presence of about 2% of the remaining adduct. All volatiles were removed under reduced pressure to give a colorless solid; the solid was redissolved in a minimal amount of toluene and stored at −30 °C for several days to give the crystalline product **15**. In a separate experiment, the reaction mixture was stirred for 15 h without taking any aliquots for NMR analysis. All volatiles were removed under reduced pressure to give a pale yellow oily solid which was washed with hexanes (2 × 2 mL) and dried, affording 0.098 g (33%) of the same product (**15**) as a pale solid.

Spectroscopic Data for the Carboxylic Acid—Borane Adduct [2,4,6-$F_3C_6H_2C(=O)OH$·$B(C_6F_5)_3$]. ^{1}H NMR (C_6D_6, 23 °C): δ 8.39 (m, 2H, Ar). ^{19}F NMR (C_6D_6, 23 °C): δ −88.10 (s br, 1F, *p*-F, $C_6H_2F_3$), −96.20 (s br, 2F, *o*-F, $C_6H_2F_3$), −137.22

(br s, 6F, *o*-F, C_6F_5), −152.03 (t, J = 19.5 Hz, 3F, *p*-F, C_6F_5), −161.54 (tt, 6F, *m*-F, C_6F_5).

Spectroscopic Data for {$(C_6F_5)_2B[OC(=O)(C_6H_2F_3)]$}$_2$ (15). ^{1}H NMR (C_6D_6, 23 °C): δ 5.67 (t, J_{H-F} = 9.0 Hz, 4H, Ar). ^{19}F NMR (C_6D_6, 23 °C): δ −88.94 (s br, 2F, *p*-F, $C_6H_2F_3$), −98.58 (s br, 4F, *o*-F, $C_6H_2F_3$), −136.08 (d, J = 15.2 Hz, 8F, *o*-F, C_6F_5), −152.99 (s br, 4F, *p*-F, C_6F_5), −162.50 (tt, 8F, *m*-F, C_6F_5).^{13}C NMR (C_6D_6, 23 °C): δ 172.35, 167.27, 163.75 ($C_6H_2F_3$, C_{ipso} obscured), 150.86, 147.62, 140.86, 113.8 (C_6F_5), 93.99 (CO(=O)).

Polymerization Procedures and Polymer Characterizations. Polymerization of propylene oxide was carried out in 50 mL Schlenk flasks on a Schlenk line. A weighed, flame-dried flask equipped with a magnet stirrer and capped with a septum was charged with propylene oxide (5.00 mL, 4.15 g, 71.5 mmol). For polymerizations employing a hydroxylic initiator, to this flask was added via microsyringe the degassed hydroxylic initiator in the desired PO/initiator ratio. After a desired temperature (23 °C) was reached using the external temperature-controlled bath, 1.0 (aluminum catalysts) or 2.0 mL (borane catalysts) of the freshly prepared catalyst solution in toluene (typically 14.3 μmol, $[PO]_0/[Cat]_0$ = 5000/1) was added into the rapidly stirred flask using a gastight syringe. (Aluminum cation **12** was generated by in situ activation of the corresponding dimethyl complex with $Ph_3CB(C_6F_5)_4$). The polymerization reactions were typically highly exothermic; the rate of catalyst addition was controlled to avoid large exotherms that would cause boiling off the monomer; a refluxing condenser was frequently used. *An external temperature-controlled bath should be used, and extra caution should be exercised when using a higher catalyst loading.* The reaction was stirred for the measured time interval, and unreacted monomer was quickly removed under reduced pressure. The residue was dried under 0.1−0.2 Torr at ambient temperatures for 2 h, yielding a viscous oil. After the polymer yield was measured, the residue was dissolved in 25 mL of methylene chloride and washed with 15 mL of 0.1 M HCl in a separatory funnel. The organic layer was washed with 2 × 10 mL distilled water and dried over anhydrous $MgSO_4$. The mixture was filtered; the solvent of the filtrate was removed in vacuo to yield oligomeric PPO, typically as a colorless, viscous oil.

For PO polymerizations with a reversed addition sequence, the catalyst solution in toluene was first mixed with a hydroxylic initiator. After the temperature was equilibrated at 23 °C, PO was added slowly over a 1.5- to 2-h period via an addition funnel. The workup procedure was identical to the polymerizations with a normal addition sequence.

All PPOs produced from this study have similar ^{1}H NMR spectra. ^{1}H NMR ($CDCl_3$, 23 °C): δ 3.8−3.2 (m, 3H, C*H*Me and C*H*$_2$), 1.2−1.0 (m, 3H, Me). PPO stereo- and regioregularities were determined by ^{13}C NMR spectroscopy according to the literature.[11,32] The relative content of the primary and secondary hydroxyl groups in the PPO products were determined with a literature method.[6c,d]

Selected PPO samples were analyzed by Matrix-assisted laser desorption/ionization time-of-flight mass spectroscopy (MALDI−TOF MS). MALDI−TOF MS was performed on a Voyager DE Pro (Perseptive Biosystems) mass spectrometer operated in linear, delayed extraction, positive ion mode using a N_2 laser at 337 nm and 20 kV accelerating voltage. Matrix 2,5-dihydroxybenzoic acid (DHBA) or dithranol in THF was mixed with NaI (aqueous solution), followed by mixing with PPO (THF solution) before this mixture was added to the target.

Gel permeation chromatography (GPC) analyses of the PPO samples were carried out at 35 °C using THF as eluent on a Waters Alliance 2690 instrument, or at 40 °C on a Waters University 1500 GPC instrument, equipped with two Polymer Laboratories 5 μm Mixed-C and one 5 μm guard columns and calibrated using monodispersed polystyrene standards at a flow rate of 1.0 mL/min. Chromatograms were processed with Polymer Laboratories GPC/SEC Cirrus software or with Waters Empower software; number-average molecular weight and polydispersity of polymers were given relative to PS standards.

Table 1. Crystal Data and Structure Refinements for 14 and 15

	14	**15**
empirical formula	$C_{29.5}H_{24}BF_{15}O_4$	$C_{45}H_{12}B_2F_{26}O_4$
fw	738.30	1132.17
temp/K	173(2)	173.2(2)
wavelength/Å	0.710 73	0.710 73
cryst syst	triclinic	monoclinic
space group	$P\bar{1}$	$P2_1/c$
a/Å	11.315(2)	13.424(2)
b/Å	11.753(2)	26.445(4)
c/Å	14.410(3)	12.5276(19)
α/deg	103.165(3)	90
β/deg	101.826(3)	105.431(3)
γ/deg	117.102(3)	90
vol/Å^3	1552.2(5)	4287.0(11)
Z	2	4
density(calcd)/(Mg/m^3)	1.580	1.754
abs coeff/mm^{-1}	0.163	0.187
F(000)	746	2232
cryst size/mm^3	0.20 × 0.18 × 0.12	0.28 × 0.25 × 0.15
θ range for data collcn/deg	3.39−23.26	3.24−20.92
index ranges	−12 ≤ h ≤ 12 −13 ≤ k ≤ 13 −15 ≤ *l* ≤ 15	−13 ≤ h ≤ 13 −26≤ k≤ 26 −12 ≤ *l* ≤ 12
no of reflcns collcd	9831	21 108
no of indep reflcns	4443 (R_{int} = 0.0716)	4528 (R_{int} = 0.1044)
data/restraints/params	4443/1/453	4528/0/695
goodness-of-fit on F^2	0.902	0.968
final R indices [$I > 2\sigma(I)$]	R_1 = 0.0656 wR_2 = 0.1895	R_1 = 0.0462 wR_2 = 0.1012
R indices (all data)	R_1 = 0.0891 wR_2 = 0.2100	R_1 = 0.0775 wR_2 = 0.1140
largest diff peak and hole/e Å^{-3}	0.964 and −0.495	0.359 and −0.205

X-ray Crystallographic Analyses of 14 and 15. Single crystals suitable for X-ray diffraction studies were obtained from slow recrystallization in toluene at −30 °C in the glovebox over a period of several days. In each case, the solvent was decanted in the glovebox, and the crystals were quickly covered with a layer of Paratone-N oil (Exxon, dried and degassed at 120 °C/10^{-6} Torr for 24 h). The crystals were then mounted on thin glass fibers and transferred into the cold-steam of a Siemens SMART CCD diffractometer. The structures were solved by direct methods and refined using the Siemens SHELXTL program library.[33] The structure was refined by full-matrix weighted least-squares on F^2 for all reflections. All non-hydrogen atoms were refined with anisotropic displacement parameters. Hydrogen atoms were included in the structure factor calculations at idealized positions unless otherwise indicated. In adduct **14**, there is a disordered toluene molecule in the lattice. Hydrogen atoms H(1) and H(2) on O(1) and O(2) were found in the difference Fourier map and their positions were refined, whereas H(3) was calculated and hydrogen for O(4) could not be located. Selected crystal data and structural refinement parameters are collected in Table 1.

Results and Discussion

PO Polymerization Catalyzed by $B(C_6F_5)_3$. Table 2 summarizes the results of PO polymerization catalyzed by $B(C_6F_5)_3$ in various $[PO]_0$:$[B]_0$:$[I]_0$ (B = $B(C_6F_5)_3$; I = hydroxylic initiator) ratios. As can be seen from the table, the use of $B(C_6F_5)_3$ alone promotes rapid ring opening reactions but produces only a mixture of low oligomers, including the dimer, trimer, and tetramer. In the presence of 15 equiv of methanol ($[PO]_0$:$[B]_0$:$[I]_0$ = 5000:1:15, entry 2), the PO polymerization produced oligomers of higher M_n (940 Da) but with high PDI (1.99). Increasing the $[I]_0$ to 30 (entry 3) resulted in a significant increase in M_n to 2900 Da and lower PDI to 1.43, despite a similar monomer conversion. Further increasing the $[I]_0$ to 120 ($[PO]_0$:$[I]_0$ = 41.7, entry 4)

Table 2. Summary of Ring-Opening Polymerization of Propylene Oxide (PO) Catalyzed by $B(C_6F_5)_3$ (B)[a]

entry	initiator (I)	$[PO]_o:[B]_o:[I]_o$ ratio	t_p (h)	yield (g)	conversion (%)	TOF[b] (10^3/h)	M_n[c] (kg/mol)	PDI
1	none	5000:1:0	2	2.22	53.5	1.34	0.17[d]	1.01
2[e]	CH_3OH	5000:1:15	2	3.23	77.8	1.94	0.94	1.99
3[e]	CH_3OH	5000:1:30	2	3.30	79.5	1.98	2.90	1.43
4[e]	CH_3OH	5000:1:120	2	3.80	91.5	2.29	2.24	1.23
5	CH_3OH	10000:1:120	0.75	1.45	34.9	4.65	1.07	1.16
6	CH_3OH	10000:1:120	1	1.60	38.5	3.85	1.15	1.16
7	CH_3OH	10000:1:120	2	2.60	62.6	3.13	1.78	1.21
8	CH_3OH	10000:1:120	4	3.49	84.1	2.10	2.32	1.28
9	H_2O	5000:1:30	4	3.25	78.3	0.98	2.99	1.41
10	H_2O	5000:1:60	2	2.36	56.9	1.42	1.54	1.22
11	H_2O	5000:1:120	2	0.62	14.9	0.37	0.33[f]	1.68
12	CH_3OH	5000:1:60	2	2.55	61.4	1.54	1.73	1.21
13	$C_6H_5CH_2OH$	5000:1:60	2	3.10	74.6	1.87	1.78	1.28
14	C_6F_5OH	5000:1:60	2	2.67	64.4	1.61	2.61	1.29
15	CF_3COOH	5000:1:60	2	2.96	71.3	1.78	0.75	1.26
16	C_6H_5COOH	5000:1:60	2	2.81	67.7	1.69	1.83	1.25
17	$2,4,6\text{-}F_3C_6H_2COOH$	5000:1:60	2	3.05	73.5	1.84	1.90	1.43
18	$HO(CH_2)_4OH$	5000:1:60	2	4.15	99.9	2.50	2.32	1.22
19[e]	$HO(CH_2)_4OH$	10000:1:120	2	3.68	88.7	2.22	2.80	1.25
20	2,5-hexanediol	5000:1:60	2	3.47	83.7	2.09	1.77	1.21
21	$HOOCC_6H_4COOH$	5000:1:60	2	2.29	55.3	1.38	3.16	1.31
22	glycerin	5000:1:15	2	3.06	73.8	1.85	3.45	1.29
23	glycerin	5000:1:30	2	3.42	82.5	2.06	3.63	1.24
24	sucrose	5000:1:15	2	2.48	59.7	1.49	3.26	1.85
25	sucrose	5000:1:30	2	2.87	69.2	1.73	2.84	1.40

[a] Carried out at 23 °C, 5.00 mL (4.15 g) of PO, with an addition sequence of monomer, initiator, and catalyst. [b] Turnover frequency (TOF) = moles of PO consumed per mole of B per hour; calculations were based on polymer yield. [c] Determined by GPC in THF against polystyrene standards. [d] Three peaks: the first peak appeared at M_n = 125, PDI = 1.00, and the third peak at M_n = 220. [e] Reverse addition (slow addition of PO to the catalyst/initiator mixture over a 1.5−2 h time period); for this addition sequence, t_p was recorded for the time used after addition of PO. [f] Three peaks.

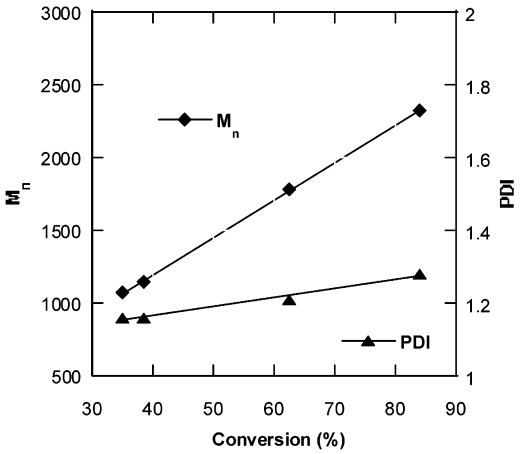

Figure 1. Plot of PPO M_n and PDI as a function of monomer conversion in a $[PO]_0:[B(C_6F_5)_3]_0$:[methanol]$_0$ ratio of 10000:1:120.

improved monomer conversion to 91.5% and raised the turnover frequency (TOF) number to 2290/h; only at this ($[PO]_0:[I]_0$ ratio does the measured molecular weight (M_n = 2240 Da, PDI = 1.23) correlate well with the calculated M_n of 2248 (M_n = 41.7 ($[PO]_0:[I]_0$ ratio) × 58.08 (M_{PO}) × 91.5% (conversion) + 32.04 ($M_{end\ group}$)).

To examine the extent of polymerization control in terms of M_n as a function of conversion, the $[PO]_0:[B]_0:[I]_0$ ratio was fixed as 10000:1:120, while polymerization time was varied to effect the monomer conversion. The polymerization results (entries 5−8) were plotted in Figure 1, showing that M_n increases linearly with an increase in monomer conversion up to 84% conversion. However, PDI also increases noticeably (from 1.16 to 1.28) as the conversion goes up; at this $[PO]_0:[I]_0$ ratio of 83.3, conversions >90% were not achieved by extending the polymerization time and the obtained M_n is much smaller than the calculated values.

Water is also an effective initiator when used in small quantities (i.e., $[PO]_0:[B]_0:[I]_0$ = 5000:1:30), producing a PPO of M_n = 2990 Da, similar to that obtained by methanol initiation under comparable conversion (entry 9 vs 3). Upon a further increase in water concentration to $[PO]_0:[B]_0:[I]_0$ = 5000:1:120, however, the polymerization activity was significantly reduced, producing only multimodal oligomers (entry 11). This reduction of activity is attributed to catalyst decomposition in high concentrations of water (vide infra).

With a fixed ratio of $[PO]_0:[B]_0:[I]_0$ = 5000:1:60 and a reaction time of 2 h, several other monofunctional hydroxylic compounds having higher Brønsted acidity, including $C_6H_5CH_2OH$ (entry 13), C_6F_5OH (entry 14), CF_3COOH (entry 15), C_6H_5COOH (entry 16), and $2,4,6\text{-}F_3C_6H_2COOH$ (entry 17), demonstrate higher activity and produce PPOs with somewhat higher molecular weight than CH_3OH (vs entry 12). An exception is CF_3COOH; despite its high activity, it produces PPOs of considerably lower molecular weight, presumably due to decomposition of the borane catalyst in CF_3COOH (vide infra). Therefore, the borane catalyst stability must be taken into account when choosing an initiator of high Brønsted acidity for better overall polymerization results.

Bifunctional initiators such as 1,4-butanediol are more effective than the above monofunctional initiators. With a ratio of $[PO]_0:[B]_0:[I]_0$ = 5000:1:60 and a 2-h reaction time, quantitative monomer conversion was observed, producing a PPO of M_n = 2320 Da with narrow molecular weight distribution (PDI = 1.22, entry 18). (Note that the $[PO]_0:[B]_0:[I]_0$ ratio of 5000:1:60 is the molar ratio; because there are two active hydrogens per diol molecular, the $[PO]_0:[-OH]_0$ ratio used for

Table 3. Summary of Ring-Opening Polymerization of Propylene Oxide Catalyzed by Other Boranes and Adducts[a]

entry	borane (B)	initiator (I)	$[PO]_o$:$[B]_o$:$[I]_o$ ratio	t_p (h)	yield (g)	conversion (%)	TOF (10^3/h)	M_n (kg/mol)	PDI
1	$B(4\text{-}F{-}C_6H_4)_3$ (**5**)	$HO(CH_2)_4OH$	5000:5:60	2	trace	0	0		
2	$B(4\text{-}F{-}C_6H_4)_3$ (**5**)	$HO(CH_2)_4OH$	5000:50:60	2	0.52	12.4	0.01		
3	$B(2,4,6\text{-}F_3{-}C_6H)_3$ (**6**)	$HO(CH_2)_4OH$	5000:1:60	2	0.71	17.0	0.43		
4	$B(C_{12}F_9)_3$ (**3**)	CH_3OH	5000:1:60	2	2.15	51.9	1.30	1.55	1.39
5	$B(C_{12}F_9)_3$ (**3**)	CH_3OH	5000:1:60	4	3.36	81.0	1.01	1.07	1.43
6	$B(C_{12}F_9)_3$ (**3**)	$HO(CH_2)_4OH$	5000:1:60	2	2.98	71.4	1.79	1.35	1.35
7	$B(C_{12}F_9)_3$ (**3**)	$HO(CH_2)_4OH$	5000:1:60	4	3.51	84.5	1.06	1.15	1.37
8	$C_2H_5CHO{\cdot}B(C_6F_5)_3$	none	5000:1:0	2	2.77	66.8	1.67	2.55	1.37
9	$C_2H_5CHO{\cdot}B(C_6F_5)_3$	CH_3OH	5000:1:60	2	3.68	88.7	2.22	1.63	1.31
10	$C_2H_5CHO{\cdot}B(C_6F_5)_3$	$HO(CH_2)_4OH$	5000:1:60	2	3.92	94.5	2.36	2.10	1.18

[a] See the footnotes in Table 2 for conditions and methods.

Table 4. Summary of Ring-Opening Polymerization of Propylene Oxide Catalyzed by Aluminum-Based Lewis Acids[a]

entry	aluminum (Al)	initiator (I)	$[PO]_o$:$[Al]_o$:$[I]_o$ ratio	t_p (h)	yield (g)	conversion (%)	TOF (10^3/h)	M_n (kg/mol)	PDI
1	$Al(OC_6F_5)_3$	none	5000:1:0	2	0.41	9.9	0.25		
2	MMAO	none	5000:50:0	2	1.93	46.4	0.02	2.97	2.47
3	PMAO (solid)	none	5000:50:0	2	3.29	79.2	0.04	4.04	1.47
4	$Al(C_6F_5)_3$	none	5000:1:0	2	2.00	48.1	1.20	0.16[b]	1.00
5	$Al(C_6F_5)_3$	CH_3OH	5000:1:60	2	2.38	57.4	1.44	0.82[c]	1.17
6	$Al(C_6F_5)_3$	$HO(CH_2)_4OH$	5000:1:60	2	0.39	9.3	0.23		
7	$Al(C_6F_5)_3$	$2,4,6\text{-}F_3C_6H_2COOH$	5000:1:60	2	trace				
8	**10**	none	5000:1:0	2	trace				
9	**11**	none	5000:1:0	2	0.11	2.7	0.07		
10	**12**	none	5000:1:0	2	2.20	53.0	1.33	10.6	1.20

[a] See the footnotes in Table 2 for conditions and methods. [b] Multiple peaks. [c] Multiple peaks: second peak appeared at $M_n = 121$, PDI = 1.00, and third peak at $M_n = 163$, PDI = 1.00.

calculating M_n by bifunctional initiators should be 41.7, rather than 83.3.) Reversing addition sequence (i.e., slow addition of PO to the catalyst/initiator mixture) resulted in lower polymer yield but higher molecular weight polymer (entry 19). Other bifunctional initiators such as 2,5-hexanediol and terephthalic acid (entries 20−21) are less effective in terms of polymerization activity, but terephthalic acid produces PPO with higher molecular weight ($M_n = 3160$ Da).

Trifunctional glycerin is the most effective initiator in the series in terms of production of PPO with the highest molecular weight ($M_n = 3630$, PDI = 1.24, entry 23), in combination with high polymerization activity. Sucrose ($f = 8$; entries 24−25) has a considerably lower activity than glycerin, presumably due to the limited solubility in PO at ambient conditions.

PO Polymerization Catalyzed by Other Boranes. To investigate the potential effect of the borane catalyst structure on polymerization characteristics, PO polymerizations were carried out using boranes varying Lewis acidity and steric bulk, the selected results of which are summarized in Table 3. Weakly Lewis acidic boranes such as BPh_3 and $B(OC_6F_5)_3$ do not produce any isolable amount of PPO, even with 50 times higher catalyst loadings. Systematically substituting hydrogen with fluorine in tris(aryl)boranes effects a gradual increase in Lewis acidity of the resulting borane, and therefore enhances PO polymerization activity correspondingly (entries 1−3, Table 3). Clearly, the PO polymerization activity trend for various boranes observed in this study correlates well with their Lewis acidity order: $B(C_6F_5)_3 > B(2,4,6\text{-}F_3{-}C_6H)_3 > B(4\text{-}F{-}C_6H_4)_3 > B(OC_6F_5)_3$, $B(Ph)_3$.[34]

The PO polymerization activity of the bulky borane PBB is comparable to that of $B(C_6F_5)_3$ when methanol is used as initiator (entries 4−5, Table 3). When 1,4-butanediol is used as initiator, PBB is less effective than $B(C_6F_5)_3$ (entries 6−7). A striking difference between the two catalysts is, however, that PBB does not isomerize PO to propionaldehyde (vide infra).

PO Polymerization Catalyzed by Aluminum-Based Lewis Acids. Table 4 summarizes the results of PO polymerization catalyzed by six different aluminum-based Lewis acids with or without a hydroxylic initiator. As can be seen from the table, $Al(OC_6F_5)_3$ has a low activity toward PO polymerization (entry 1); addition of an initiator such as 1,4-butanediol diminishes the activity. MMAO has appreciable polymerization activity (TOF = 20/h), producing PPO of $M_n = 2970$ Da but with a broad molecular weight distribution of 2.47 (entry 2). On the other hand, solid PMAO substantially free of trialkylaluminum produced PPO of higher molecular weight ($M_n = 4040$ Da) and narrower molecular weight distribution (PDI = 1.47, entry 3) and exhibited higher activity as well (TOF = 40/h).

The highly Lewis acidic alane $Al(C_6F_5)_3$ is very reactive toward PO, but produces only a mixture of low oligomers, including the dimer, trimer, and tetramer (entry 4). Addition of methanol in a ratio of $[PO]_0$:$[Al]_0$:$[I]_0 = 500:1:60$ improved monomer conversion but still produced low molecular weight oligomers (entry 5). The use of 1,4-butanediol resulted in a sharp decrease in polymerization activity (entry 6). Not surprisingly, carboxylic acid initiator $2,4,6\text{-}F_3C_6H_2COOH$ completely shut down the activity of the alane (entry 7), due to decomposition of the alane catalyst in the presence of strong Brønsted acids. Monomeric aluminum alkyls supported by the [N⁀N] dichelating ligand such as neutral, three-coordinate aluminum complex **10**, are inactive for PO polymerization, while the dimeric, four-coordinate aluminum complex **11** has noticeable activity in the absence of hydroxylic initiator (entries 8−9).

Three-coordinate methyl aluminum cation **12**,[30a] which can be generated by in situ activation of the four-

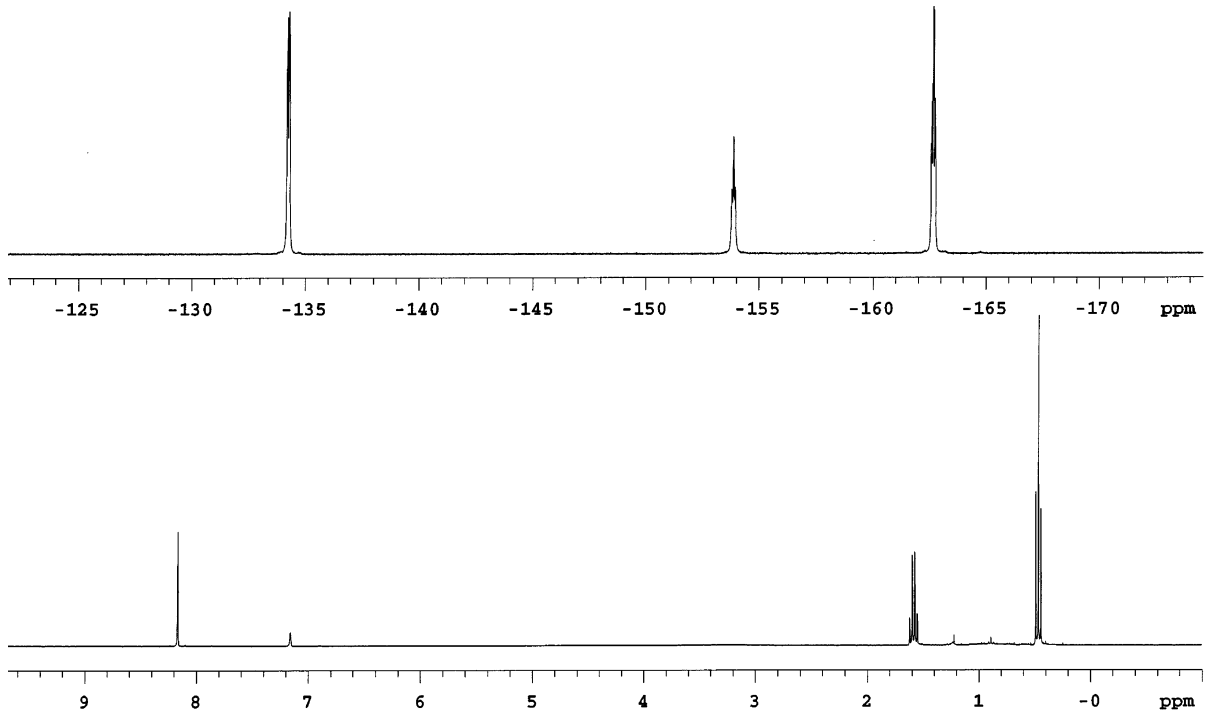

Figure 2. NMR spectra of $CH_3CH_2CHO{\cdot}B(C_6F_5)_3$, formed from the PO isomerization in the presence of $B(C_6F_5)_3$ (top spectrum, ^{19}F; bottom spectrum, ^1H (peak at δ 7.15 ppm for benzene-d_6 NMR solvent; a small amount of residual hexanes shown at δ 1.22, 0.88 ppm).

coordinate β-diketiminate dimethyl aluminum precursor with $Ph_3CB(C_6F_5)_4$, exhibits considerable activity for PO polymerization, giving a high TOF number of 1340/h and producing high molecular weight PPO (M_n = 10 600 Da, PDI = 1.20, entry 10, Table 4). As compared to other cationic aluminum complexes that vary in coordination number from 3 to 6 reported in the literature,[16−19] three-coordinate aluminum cation **12** is most reactive and also produces PPO with the highest molecular weight. However, the catalytic activity of the cation completely vanishes when used in combination with hydroxylic initiators.

PO Isomerization by $B(C_6F_5)_3$. Rearrangement of epoxides can be effected by many reagents, most noticeably protic or Lewis acids and bases.[35] Isomerization of epoxides to carbonyl compounds is typically carried out with acid catalysis, whereas isomerization to allylic alcohols is usually carried out with base-catalyzed reactions. To investigate the possible isomerization of PO by $B(C_6F_5)_3$ with or without a hydroxylic initiator, the reaction was monitored by NMR spectroscopy; isolation of the product was also carried out.

Monitoring the NMR-scale reaction of PO with the borane in toluene at various [PO]:[Borane] ratios by both ^1H and ^{19}F NMR revealed the formation of propionaldehyde (observed as a borane adduct: $CH_3CH_2CHO{\cdot}B(C_6F_5)_3$) and oligomeric products. Scale-up reactions in toluene starting from low temperature also resulted in similar mixtures. Under the same conditions, the reaction of PO with $B(C_6F_5)_3$ in hexanes produced the propionaldehyde−borane adduct which was subsequently isolated (Figure 2). This PO isomerization catalyzed by the borane is highly regioselective; it forms exclusively propionaldehyde and no acetone. The overall reaction involving a hydride shift for the formation of $CH_3CH_2CHO{\cdot}B(C_6F_5)_3$ is proposed in eq 2. Interestingly, formation of $CH_3CH_2CHO{\cdot}B(C_6F_5)_3$ was substantially suppressed in the reaction of PO with borane·methanol adduct $(C_6F_5)_3B{\cdot}HOMe$ in hexanes; the same reaction with $(C_6F_5)_3B{\cdot}2HOMe$ produced the desired PPO oligomers with only a trace amount of the propionaldehyde−borane adduct being detected.

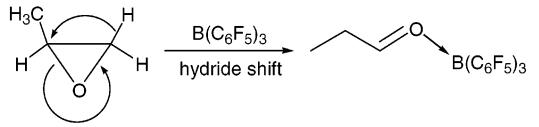

(2)

The presence of $CH_3CH_2CHO{\cdot}B(C_6F_5)_3$ in the PO polymerization system can lead to production of acetals ($CH_3CH_2CH(OR)_2$) or hemiacetals ($CH_3CH_2CH(OH)(OR)$) when the propionaldehyde−borane adduct reacts with hydroxylic initiators or directly with the PO oligomer; therefore, formation of such an adduct is undesirable to the PO polymerization process. However, the formation of the propionaldehyde−borane adduct is not a catalyst decomposition (or poisoning) pathway because this adduct can catalyze a rapid PO polymerization with or without added hydroxylic initiator (entries 8−10, Table 3). The PO polymerizations catalyzed by the propionaldehyde−borane adduct using methanol or 1,4-butanediol initiators rival those catalyzed by $B(C_6F_5)_3$; more interestingly, in the absence of added hydroxylic initiator, this adduct also produced PPO of M_n = 2550 (PDI = 1.37) with good activity (TOF = 1670/h), whereas the PO polymerization catalyzed by $B(C_6F_5)_3$ alone produced only a mixture of low oligomers (vide supra).

A potential strategy for suppressing the PO isomerization in the polymerization process is to employ the borane catalysts exhibiting lower Lewis acidity. However, these boranes have little or no activity for PO polymerization (vide supra). Sterics of the borane catalyst seem to solve this problem; the bulky borane PBB does not isomerize PO to propionaldehyde in stoichiometric or polymerization reactions in the presence or

Scheme 4

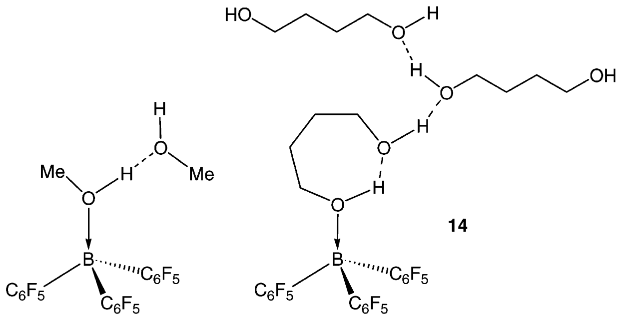

Scheme 5

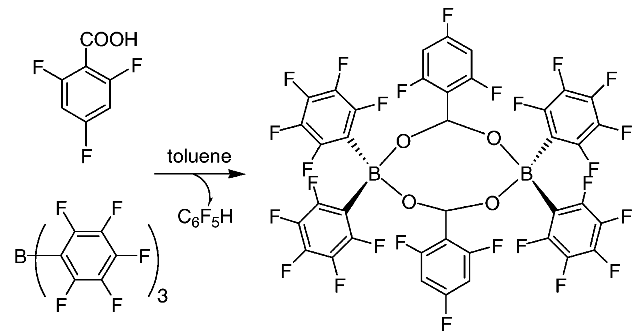

15

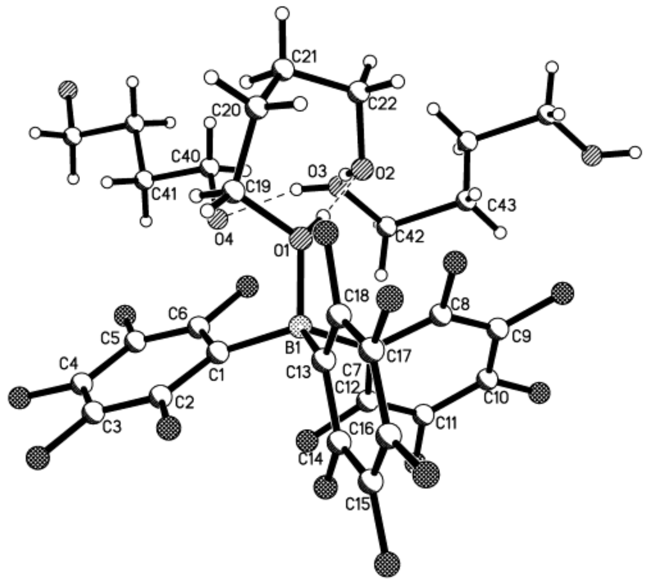

Figure 3. X-ray crystal structure of **14**.

in the absence of initiators, but it still exhibits comparable polymerization activity to that catalyzed by $B(C_6F_5)_3$ in some cases.

Reaction of $B(C_6F_5)_3$ with Hydroxylic Initiators. $B(C_6F_5)_3$ is known to form stable 1:1 or 1:2 adducts with monofunctional alcohols, drastically increasing acidity of otherwise weakly Brønsted acidic alcohols.[36] A stability study of these adducts showed no sign of catalyst decomposition in hydrocarbon or ether solvents. Reaction of $B(C_6F_5)_3$ with bifunctional initiators such as 1,4-butanediol also produces stable adducts. Depending on the reactant ratio and reaction conditions (see Experimental Section), the NMR spectroscopic data for the isolated adducts reveal the presence of two types of 1,4-butanediol molecules in either a 1:1 or a 1:2 ratio, suggesting a 1:2 borane/diol adduct $HO(CH_2)_4OH{\cdot}OH(CH_2)_4HO{\cdot}B(C_6F_5)_3$ (**13**) and a 1:3 borane/diol adduct $2HO(CH_2)_4OH{\cdot}OH(CH_2)_4HO{\cdot}B(C_6F_5)_3$ (**14**), respectively. Both the inner diol (datively bonded to the borane) and outer diol (hydrogen-bonded to the inner diol) molecules in **13** and **14** exhibit methylene protons that are considerably high-field shifted as compared to the uncomplexed 1,4-butanediol (δ 3.63 (α) and 1.64 (β) ppm), however, such shift for the methylene protons of the inner diol molecule is more pronounced (δ 2.55 (α) and 0.66 (β) ppm for **13**; δ 2.90 (α) and 0.87 (β) ppm for **14**). For 1:3 borane/diol adduct **14**, the two outer diol molecules are indistinguishable in NMR spectroscopy at ambient temperature (δ 3.07 (α) and 1.15 (β) ppm); however, the structure of this adduct has been confirmed by X-ray diffraction studies (vide infra). For comparison, Scheme 4 depicts two representative borane−alcohol adduct structures: on the left is an adduct of the borane with a monofunctional alcohol ($[(C_6F_5)_3B{\cdot}OHMe]{\cdot}HOMe$);[36a] on the right is an adduct of the borane with a bifunctional alcohol (**14**).

Excess of water and certain carboxylic acids cause a decrease in catalyst activity of $B(C_6F_5)_3$ (see Table 2). To investigate a possible catalyst decomposition pathway, the stoichiometric reaction of $B(C_6F_5)_3$ and 2,4,6-$F_3C_6H_2COOH$ was carried out in toluene (see Experimental Section). Stirring the reaction mixing at −30 °C for 45 min afforded the desired carboxylic acid−borane adduct [2,4,6-$F_3C_6H_2C({=}O)OH{\cdot}B(C_6F_5)_3$] as the minor fraction (28%), but a new species as the major product (72%). After the reaction being stirred for an extended time, the new species was isolated and spectroscopically characterized as a borane dimer $\{(C_6F_5)_2B[OC({=}O)(C_6H_2F_3)]\}_2$ (**15**, Scheme 5), the formation of which is presumably driven by elimination of pentafluorobenzene. The molecular structure of **15** has been confirmed by X-ray diffraction studies (vide infra). Decomposition of $B(C_6F_5)_3$ with CF_3COOH is even more pronounced; extensive reaction occurs immediately upon mixing these two reagents in hexanes, producing large precipitates. This solid product is insoluble in C_6D_6 and further characterizations were not performed.

X-ray Crystal Structures of $2HO(CH_2)_4OH{\cdot}OH(CH_2)_4HO{\cdot}B(C_6F_5)_3$ (14) and $\{(C_6F_5)_2B[OC({=}O)(C_6H_2F_3)]\}_2$ (15). The molecular structures of complexes **14** and **15** in their solid states are confirmed by X-ray diffraction studies and shown in Figures 3 and 4, respectively. Important bond distances and angles for these two complexes are tabulated in Tables 5 and 6.

Complex **14** crystallizes in the triclinic space group $P\bar{1}$. In the solid state, there are three 1,4-butanediol molecules per borane molecule in **14**; the first is coordinated through dative bonding between oxygen and boron, while the second and the third are linked together via O−H···O hydrogen bonding. In the dative bonding site, the geometry at boron is a distorted tetrahedron with the sum of the C−B−C angles of 336.0°, whereas O(1) adopts a trigonal pyramidal geometry, which suggests that only one lone pair from the alcohol oxygen atom is employed in the bonding to boron. This is in sharp contrast to the bonding mode observed for $(C_6F_5)_3Al{\cdot}OHMe$ in which oxygen has a trigonal-planar geometry, implying that both lone pairs from the oxygen atom are employed in the bonding to aluminum.[37] The average B−C(aryl) distance (1.645 Å) in **14** compares well to other $(C_6F_5)_3B$ complexes with water and/or alcohol, such as $(C_6F_5)_3B{\cdot}OH_2$,[38] $(C_6F_5)_3B{\cdot}2OH_2$,[39] $[(C_6F_5)_3B{\cdot}OH_2]{\cdot}HOBu^t$,[36a] and $[(C_6F_5)_3B{\cdot}OHMe]{\cdot}HOMe$,[36a] but the B−O distance (1.535(5) Å) is notice-

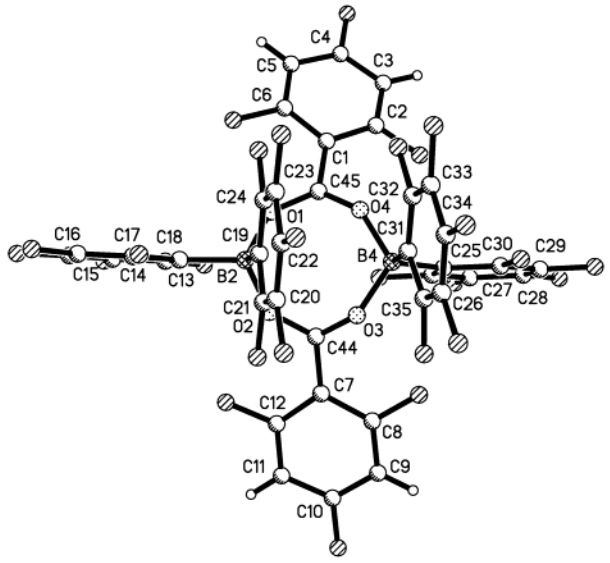

Figure 4. X-ray crystal structure of **15**.

Table 5. Selected Bond Distances (Å) and Bond Angles (deg) for 14

B(1)−O(1)	1.535(5)	B(1)−C(1)	1.632(6)
B(1)−C(7)	1.659(6)	B(1)−C(13)	1.643(6)
O(1)−C(19)	1.462(5)	O(2)−C(22)	1.449(5)
O(1)−H(1)	0.90(5)	H(1)···O(2)	1.52(5)
O(1)···O(2)	2.413(4)	O(2)−H(2)	0.80(5)
H(2)···O(3)	1.80(5)	O(2)···O(3)	2.572(5)
H(3)···O(4)	1.91(2)		
O(1)−B(1)−C(1)	106.6(3)	O(1)−B(1)−C(7)	103.7(3)
O(1)−B(1)−C(13)	110.0(3)	C(1)−B(1)−C(7)	113.8(3)
C(1)−B(1)−C(13)	116.1(3)	C(7)−B(1)−C(13)	106.1(3)
O(1)−H(1)···O(2)	170(4)	O(2)−H(2)···O(3)	162(5)
O(3)−H(3)···O(4)	161(5)		

Table 6. Selected Bond Distances (Å) and Bond Angles (deg) for 15

B(2)−O(1)	1.525(2)	B(2)−O(2)	1.507(5)
B(4)−O(3)	1.502(2)	B(4)−O(4)	1.532(5)
B(2)−C(13)	1.604(6)	B(2)−C(19)	1.617(6)
B(4)−C(25)	1.614(6)	B(4)−C(31)	1.592(6)
C(44)−O(2)	1.273(4)	C(44)−O(3)	1.260(5)
C(45)−O(1)	1.263(4)	C(45)−O(4)	1.248(4)
O(1)−B(2)−O(2)	105.2(3)	O(3)−B(4)−O(4)	112.3(3)
O(1)−C(45)−O(4)	126.0(4)	O(2)−C(44)−O(3)	124.4(4)
B(2)−O(1)−C(45)	129.4(3)	B(2)−O(2)−C(44)	128.5(3)
B(4)−O(3)−C(44)	144.1(3)	B(4)−O(4)−C(45)	148.0(3)
O(1)−B(2)−C(13)	104.6(3)	O(1)−B(2)−C(19)	111.6(3)
O(2)−B(2)−C(13)	106.2(3)	O(2)−B(2)−C(19)	113.0(3)
C(13)−B(2)−C(19)	115.4(3)	O(3)−B(4)−C(25)	107.1(3)
O(3)−B(4)−C(31)	108.5(3)	O(4)−B(4)−C(25)	103.6(3)
O(4)−B(4)−C(31)	108.0(3)	C(25)−B(4)−C(31)	117.4(3)

ably shorter than that in the other complexes. The first 1,4-butanediol molecule forms a seven-membered O−H···O−C−C−C−C ring through intramolecular O(1)−H(1)···O(2) hydrogen bonding, with the ring adopting a chair conformation. Hydrogen atoms H(1) and H(2) on O(1) and O(2) were found in the difference Fourier map and their positions were refined. A relatively short H(1)···O(2) bond distance of 1.52(5) Å and a large O(1)−H(1)···O(2) angle of 170(4)° are indicative of moderately strong hydrogen bonding.[40] Relatively weaker O(2)−H(2)···O(3) and O(3)−H(3)···O(4) hydrogen bonds link the second and the third 1,4-butanediol molecules together.

Dimeric complex **15** crystallizes in the monoclinic space group $P2_1/c$; two $(C_6F_5)_2B$ centers are connected unsymmetrically via two 2,4,6-$F_3C_6H_2C(=O)O$ bridging groups. The geometry at the boron centers is distorted tetrahedral, whereas both bridging aryl carbons are trigonal planar (i.e., the sums of the angles around C(44) and C(45) are 359.9 and 360.1°, respectively) and are subsequently sp^2-hybridized. Interestingly, two 2,4,6-F_3Ph groups on the bridge are both slightly tilted to the same side (i.e., toward the B(4) center). The average B−C(aryl) distance (1.607 Å) is shorter by ∼0.04 Å than that in complex **14** where there are three C_6F_5 groups bonded to boron. The two B−O bonds at each boron are unsymmetrical and they differ from each other by 0.02 and 0.03 Å, respectively, while the two C−O bonds at each bridging carbon ((C(44) and C(45) are only slightly unsymmetrical. The central eight-membered ring adopts a crown type of conformation.

Structures of PPOs Produced by Boron and Aluminum Lewis Acids. All PPOs produced by the borane catalyst are atactic and regioirregular, according to the analysis by ^{13}C NMR spectroscopy. The relative content of the primary vs secondary hydroxyl groups in the PPO products were determined by the esterification of the hydroxyl groups with an excess of $(CF_3CO)_2O$ in $CDCl_3$, followed by measuring the integrals of the methylene proton in the form of $CF_3COOCH_2CH(CH_3)-$ (d, 4.20 ppm) and the methine proton in the form of $CF_3COOCH(CH_3)CH_2-$ (sextet, 5.15 ppm), using ^1H NMR spectroscopy according to the literature method.[6c,d] For PPOs produced by the borane catalyst in combination with initiators such as methanol, water, and carboxylic acids, the relative content of the primary and secondary hydroxyl groups is about equal; the PPO produced by the aluminum cation (**12**) exhibits the same ratio. However, the borane/1,4-butanediol and borane/glycerin catalyst systems produce PPOs having higher primary hydroxyl contents with a typical [primary OH]/[secondary OH] ratio ≥60/40, reflecting a noticeable preference in breaking the oxygen−methine bond over the oxygen−methylene bond in the ring-opening process by these two catalyst systems and therefore producing more primary hydroxyl end groups.

Four selected PPO samples were analyzed by MALDI−TOF MS to examine the influence of initiator and addition sequence on PPO and end group structures; these PPOs are produced by $B(C_6F_5)_3$/1,4-butanediol (Table 2, entry 18), $B(C_6F_5)_3$/1,4-butanediol with reversed addition (Table 2, entry 19), $B(C_6F_5)_3$/2,4,6-$F_3C_6H_2COOH$ (Table 2, entry 17), and by aluminum cation **12** (Table 4, entry 12).

Figure 5 depicts a selected range of the MALDI−TOF MS spectrum of the PPO prepared with $B(C_6F_5)_3$/1,4-butanediol. There are two primary mass distributions, both of which have mass differences between the peaks representing the molar mass of PO (58.08 g/mol). The distribution with higher intensities (**A** series) in Figure 5 represents the liner PO structure **A** shown in Scheme 6, where $M_{\text{end group}}$ is the molar mass of 1,4-butanediol initiator (M = 90.12) and n is the degree of polymerization. The calculated mass values (e.g., M_{23} = 1448.95 Da) correlates well with the measured mass values (e.g., M_{23} = 1449.03 Da) listed in Figure 5. The second PO structure is identified as linear structure **B** where $M_{\text{end group}}$ is the molar mass of water molecule (M = 18.02), the mass distribution of which is labeled as **B** series in Figure 5. The calculated (e.g., M_{24} = 1434.93 Da) and the found (M_{24} = 1435.06 Da) mass values match well. The formation of such a secondary structure

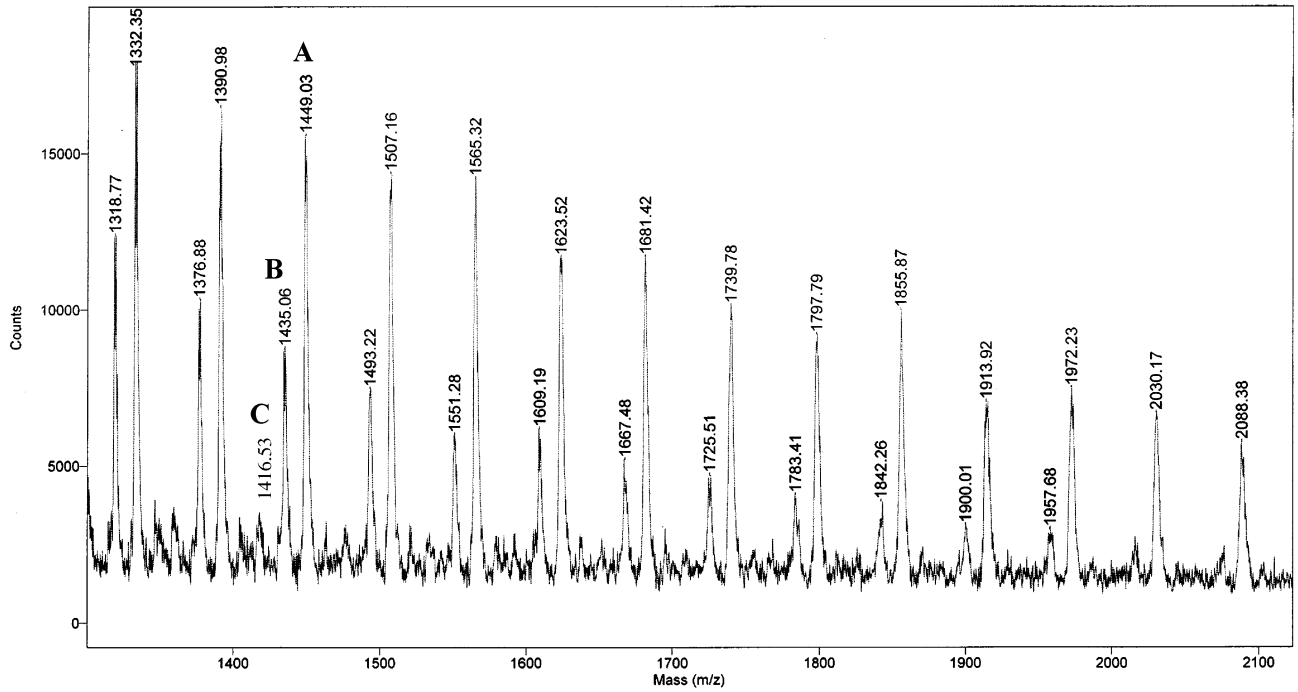

Figure 5. Selected range of the MALDI−TOF MS spectrum of the PPO produced by $B(C_6F_5)_3$/1,4-butanediol with **A**, **B**, and **C** representing the mass distributions for the three PO structures shown in Scheme 6.

Scheme 6

A: RO−[$(C_3H_6O)_n$]−H $M_n = (C_3H_6O)_n + M_{end\ group} + M^+_{Na}$

M_{23} = 1448.95 Da $= (58.08) \times n + 113.11$

B: HO−[$(C_3H_6O)_n$]−H $M_n = (C_3H_6O)_n + M_{end\ group} + M^+_{Na}$

M_{24} = 1434.93 Da $= (58.08) \times n + 41.01$

C: [$(C_3H_6O)_n$] $M_n = (C_3H_6O)_n + M^+_{Na}$

M_{24} = 1416.91 Da $= (58.08) \times n + 22.99$

can be attributed to two pathways: initiation by water contained in 1,4-butanediol and proton-initiated cationic ring-opening of PO. A small amount of cyclic PO structure **C** is also identified as **C** mass distribution series in Figure 5, with good agreement between the calculated (e.g., M_{24} = 1416.91 Da) and the measured (M_{24} = 1416.53 Da) mass values.

The MALDI−TOF MS spectrum of the PPO sample prepared with $B(C_6F_5)_3$/1,4-butanediol in reversed addition also features two major mass distributions for linear PPO structures **A** and **B** and a minor mass distribution for cyclic structure **C**, the spectrum of which is depicted in Figure 6. Using the same equations in Scheme 6, the calculated mass values for peaks **A**, **B**, and **C** match well with the measured values marked in Figure 6. The MALDI−TOF MS spectrum of the PPO sample prepared with $B(C_6F_5)_3$/2,4,6-$F_3C_6H_2COOH$ shows similarly the three types of PPO structures.

The MALDI−TOF MS spectrum of the PPO sample prepared with aluminum cation **12** reveals four distinct mass distribution series representing four PPO structures **A**−**D** (Figure 7). Linear structure **B** with −H and −OH as end groups is seen as the primary distribution, as anticipated as a result of cationic ROP directly initiated by aluminum cation **12**. The calculated mass for n = 24 of this structure is 1434.91 Da, which agrees well with the experimental value of M_{24} = 1434.21 Da. The cyclic PO structure is identified as **C** distribution series in Figure 7 (e.g., the calculated M_{25} = 1474.99 Da; the found M_{25} = 1475.21 Da). The **D** distribution series can be attributed to structure **D** (Ph_3C−[(O-$C_3H_6)_n$]−Cl; e.g., the calculated M_{20} = 1463.37 Da, the found M_{24} = 1462.31 Da), presumably as a result of initiation by excess or unreacted activator $Ph_3CB(C_6F_5)_4$ used for generating **12** by in situ activation and termination by CH_2Cl_2 and/or HCl (see Experimental Section). Interestingly, the unexpected structure **A** with −H and −OMe end groups are also seen, as evidenced by good agreement between the calculated (e.g., M_{24} = 1448.95 Da) and the found (M_{24} = 1448.40 Da) mass values. The formation of type **A** structure can be attributed to transformation of the Al−Me bond to Al−OMe by adventitious oxygen or other possible decomposition pathways, followed by nucleophilic attack of the activated PO by the OMe group, possibly in a bimetallic fashion.

Conclusions

The highly Lewis acidic, chemically robust organoborane $B(C_6F_5)_3$, when combined with hydroxylic initiators, catalyzes rapid ring-opening polymerization of PO to produce PPOs having low to medium molecular weights and narrow molecular weight distributions. In the absence of hydroxylic initiator, $B(C_6F_5)_3$ predominantly catalyzes isomerization of PO to propionaldehyde in hexanes and produces a mixture of low oligomers and propionaldehyde in toluene. Addition of sufficient high concentration of hydroxylic initiator in terms of $[PO]_0$:$[-OH]_0$ ratio is most critical for achieving polymerization control.

The PO polymerization activity is proportional to Lewis acidity of the borane catalyst and Brønsted acidity of the hydroxylic initiator. However, excess of water and carboxylic acid initiators deactivates the borane catalyst, resulting in lower catalytic activity. Decomposition of the borane is believed to occur through elimination of pentafluorobenzene. On the other hand, the borane catalyst is very stable toward alcohol initiators. The spectroscopic data and structural features for the bo-

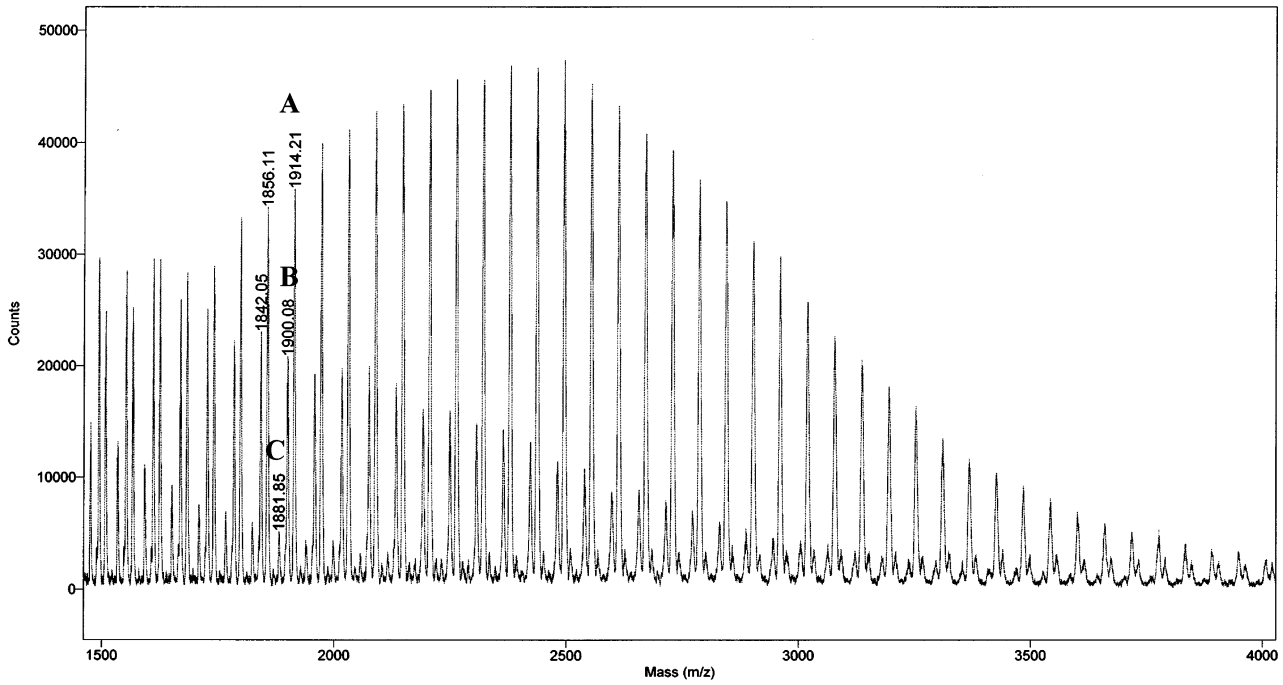

Figure 6. Selected range of the MALDI−TOF MS spectrum of the PPO produced by $B(C_6F_5)_3$/1,4-butanediol under the reversed addition sequence with **A**, **B**, and **C** representing the mass distributions for the three PO structures shown in Scheme 6.

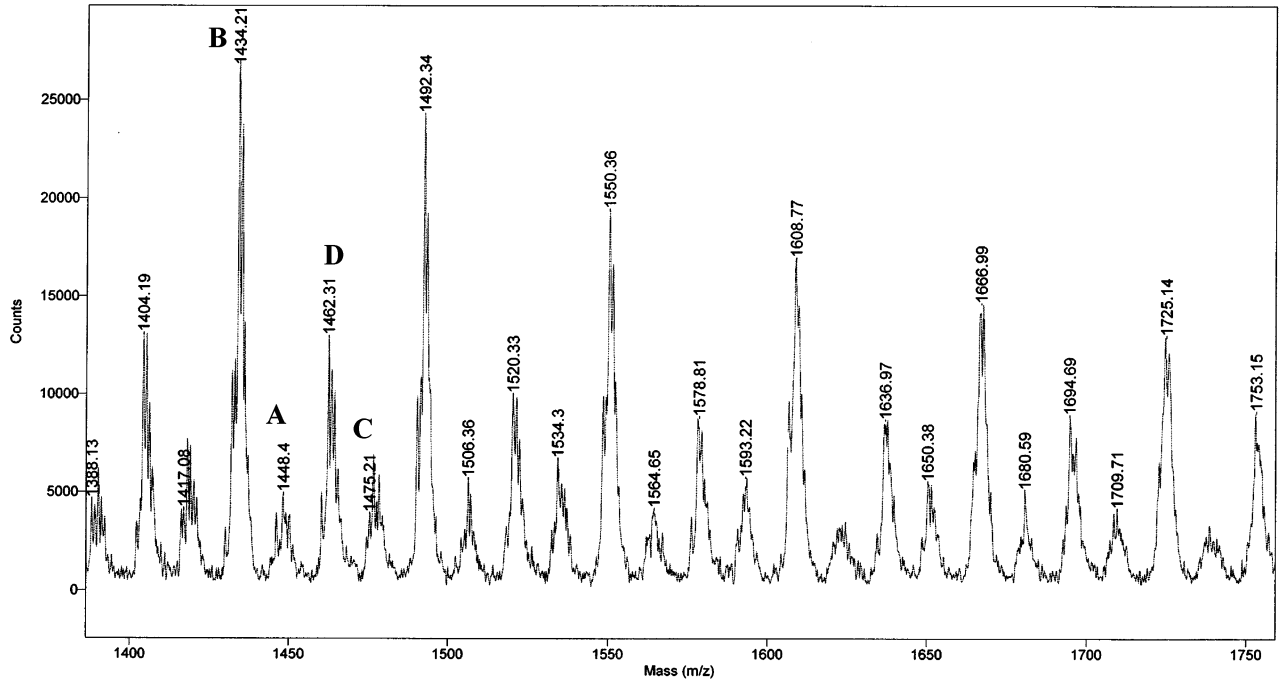

Figure 7. Selected range of the MALDI−TOF MS spectrum of the PPO produced by cationic aluminum complex **12** with **A**−**D** representing the mass distributions for four different PO structures.

rane:diol adducts indicate strong activation of the weak Brønsted acid by $B(C_6F_5)_3$.

The neutral aluminum Lewis acids investigated in this study are much less effective in PO polymerization than the boranes. The analogous alane $Al(C_6F_5)_3$ catalyzes facile PO oligomerization; however, its application in PO polymerization is substantially limited due to its instability toward hydroxylic initiators. PMAO substantially free of trialkylaluminums exhibits low polymerization activity but produces PPO of relatively high molecular weight (M_n > 4000). The three-coordinate aluminum cation **12** exhibits good activity and also produces PPO with the highest molecular weight (M_n > 10 000) in the series, although the MALDI−TOF MS analysis of the PPO product reveals three linear chain structures, in addition to a cyclic structure.

All PPOs produced by the borane catalyst are atactic and regioirregular. In addition to the presence of two linear PPO structures having the initiator and water molecules as end groups, a small amount of cyclic PPO is also seen in these products. The relative contents of the primary vs the secondary hydroxyl group are about equal for monofunctional initiators; however, diol and triol initiators produce PPOs having higher primary hydroxyl contents with a typical [primary OH]/[secondary OH] ratio ≥60/40. Overall, the most effective

catalyst is $B(C_6F_5)_3$, initiators are diols and triols, and the $[PO]_0:[-OH]_0$ ratio is 41.7, as judged by polymerization activity, catalyst stability, and the ability to produce PPOs with desired molecular weights.

Acknowledgment. This work was supported by The Dow Chemical Co. We thank W. Jack Kruper, Pete N. Nickias, and John Weston of Dow Chemical for helpful discussions and Ms. Susie M. Miller for the X-ray diffraction analyses. E.Y.-X.C. gratefully acknowledges an Alfred P. Sloan Research Fellowship.

Supporting Information Available: CIF file containing crystallographic data for **14** and **15**. This material is available free of charge via the Internet at http://pubs.acs.org.

References and Notes

(1) (a) Gagnon, S. D. In *Kirk-Othmer Encyclopedia of Chemical Technology*, 4th ed.; Kroschwitz, J. I.; Howe-Grant, M., Eds.; John Wiley and Sons: New York, 1996; Vol. 19, pp 722−743. (b) Gagnon, S. D. In *Encyclopedia of Polymer Science and Engineering*, 2nd ed.; Kroschwitz, J. I., Ed.; John Wiley and Sons: New York, 1986; Vol. 6, pp 273−307.

(2) (a) Szycher, M. *Handbook of Polyurethanes*; CRC Press: New York, 1994. Oertel, G. *Polyurethane Handbook: Chemistry, Raw Materials, Processing, Application, Properties*, 2nd ed.; Hanser-Gardner Pubns: Cincinnati, OH, 1994.

(3) Sparrow, D. J.; Thorpe, D. In *Telechelic Polymers: Synthesis and Applications*; Goethals, E. J., Ed.; CRC Press: Boca Raton, FL, 1989; pp 181−228.

(4) Kubisa, P. In *Cationic Polymerizations: Mechanisms, Synthesis, and Applications*; Matyjaszewski, K., Ed.; Marcel Dekker: New York, 1996; pp 437−553.

(5) (a) Goethals, E. J. *Adv. Polym. Sci.* **1977**, *23*, 103−130. (b) Katnik, R. J.; Schaefer, J. *J. Org. Chem.* **1968**, *33*, 384−388. (c) Kern, R. J. *J. Org. Chem.* **1968**, *33*, 388−390.

(6) (a) Penczek, S. *J. Polym. Sci., Part A: Polym. Chem.* **2000**, *38*, 1919−1933. (b) Kubisa, P.; Penczek, S. *Prog. Polym. Sci.* **1999**, *24*, 1409−1437. (c) Bednarek, M.; Kubisa, P.; Penczek, S. *Makromol. Chem. Suppl.* **1989**, *15*, 49−60. (d) Wojtania, M.; Kubisa, P.; Penczek, S. *Makromol. Chem. Macromol. Symp.* **1986**, *6*, 201−206.

(7) For representative reviews, see: (a) Sugimoto, H.; Inoue, S. *Adv. Polym. Sci.* **1999**, *146*, 39−119. (b) Kuran, W. *Prog. Polym. Sci.* **1998**, *23*, 919−992.

(8) Pruitt, M. E.; Baggett, M. M. U.S. Patent, 2,706,181, 1955.

(9) (a) Aida, T.; Inoue, S. *Acc. Chem. Res.* **1996**, *29*, 39−48. (b) Sugimoto, H.; Kawamura, C.; Kuroki, M.; Aida, T.; Inoue, S. *Macromolecules* **1994**, *27*, 2013−2018. (c) Aida, T.; Maekawa, Y.; Asano, S.; Inoue, S. *Macromolecules* **1988**, *21*, 1195−1202. (d) Aida, T.; Inoue, S. *Macromolecules* **1981**, *14*, 1166−1169.

(10) (a) Le Borgne, A.; Vincens, V.; Jouglard, M.; Spassky, N. *Macromol. Symp.* **1993**, *73*, 37−46. (b) Vincens, V.; Le Borgne, A.; Spassky, N. *Macromol. Chem. Rapid Commun.* **1989**, *10*, 623−628. (c) Le Borgne, A.; Spassky, N.; Jun, C. L.; Momtaz, A. *Macromol. Chem.* **1988**, *189*, 637−650.

(11) Antelmann, B.; Chisholm, M. H.; Iyer, S.; Huffman, J. C.; Navarro-Llobet, D.; Pagel, M.; Simonsick, W. J.; Zhong, W. *Macromolecules* **2001**, *34*, 3159−3174.

(12) (a) Vandenberg, E. J. *J. Polym. Sci., Part A-1* **1969**, *7*, 525−567. (b) Vandenberg, E. J. *J. Polym. Sci.* **1960**, *47*, 489−491.

(13) Colclough, R. O.; Wilkinson, K. *J. Polym. Sci., Part C* **1964**, *4*, 311−332.

(14) Wu, B.; Harlan, C. J.; Lenz, R. W.; Barron, A. R. *Macromolecules* **1997**, *30*, 316−318.

(15) (a) Huang, Y.-J.; Zi, G.-R.; Wang, Y.-H. *J. Polym. Sci., Part A: Polym. Chem.* **2002**, *40*, 1142−1150. (b) O'Connor, J. M.; Lickei, D. L.; Grieve, R. L. U.S. Patent 6,359, 101, 2002. (c) Hofmann, J.; Ooms, P.; Gupta, P.; Schafer, W. U.S. Patent 6,291,388, 2001. (d) Le-Khac, B. U.S. Patent 6,211,330, 2001. (e) Ooms, P.; Hofmann, J.; Gupta, P.; Groenendaal, L. U.S. Patent 6,204,357, 2001. (f) Le-Khac, B. U.S. Patent 5,482,-908, 1996.

(16) (a) Munoz-Hernandez, M.-A.; Mckee, M. L.; Keizer, T. S.; Yearwood, B. C.; Atwood, D. A. *J. Chem. Soc., Dalton Trans.* **2002**, 410−414. (b) Jegier, J. A.; Munoz-Hernandez, M.-A.; Atwood, D. A. *J. Chem. Soc., Dalton Trans.* **1999**, 2583−2587. (c) Munoz-Hernandez, M.-A.; Sannigrahi, B.; Atwood, D. A. *J. Am. Chem. Soc.* **1999**, *121*, 6747−6748. (d) Wei, P.; Atwood, D. A. *Inorg. Chem.* **1998**, *37*, 4934−4938.

(17) Baugh, L. S.; Sissano, J. A. *J. Polym. Sci., Part A: Polym. Chem.* **2002**, *40*, 1633−1651.

(18) Korolev, A. V.; Ihara, E.; Guzei, I. A.; Young, V. G., Jr.; Jordan, R. F. *J. Am. Chem. Soc.* **2001**, *123*, 8291−8309.

(19) Emig, N.; Nguyen, H.; Krautscheid, H.; Reau, R.; Cazaux, J.-B.; Bertrand, G. *Organometallics* **1998**, *17*, 3599−3608.

(20) Braune, W.; Okuda, J. *Angew. Chem., Int. Ed.* **2003**, *42*, 64−68.

(21) (a) Chien, J. C. W.; Tsai, W.-M.; Rausch, M. D. *J. Am. Chem. Soc.* **1991**, *113*, 8570−8571. (b) Ewen, J. A.; Elder, M. J. Eur. Pat. Appl. EP 0,426,637, 1991.

(22) Naumann, D.; Butler, H.; Gnann, R. *Z. Anorg. Allg. Chem.* **1992**, *618*, 74−76.

(23) Chen, Y.-X.; Metz, M. V.; Li, L.; Stern, C. L.; Marks, T. J. *J. Am. Chem. Soc.* **1998**, *120*, 6287−6305.

(24) Feng, S.; Roof, G. R.; Chen, E. Y.-X. *Organometallics* **2002**, *21*, 832−839.

(25) Biagini, P.; Lugli, G.; Abis, L.; Andreussi, P. U. S. Pat. 5,-602,269, 1997.

(26) Chakraborty, D.; Chen, E. Y.-X. *Macromolecules* **2002**, *35*, 13−15.

(27) Smith, G. M.; Palmaka, S. W.; Rogers, J. S.; Malpass, D. B.; Monfiston, D. J. PCT, WO 97/23288, 1997.

(28) Chakraborty, D.; Chen, E. Y.-X. *Organometallics* **2002**, *21*, 1438−1442.

(29) Chakraborty, D.; Chen, E. Y.-X. *Organometallics* **2003**, *22*, 769−774.

(30) (a) Radzewich, C. E.; Guzei, I. A.; Jordan, R. F. *J. Am. Chem. Soc.* **1999**, *121*, 8673−8674. (b) Radzewich, C. E.; Coles, M. P.; Jordan, R. F. *J. Am. Chem. Soc.* **1998**, *120*, 9384−9385. (c) Qian, B.; Ward, D. L.; Smith, M. R.; III. *Organometallics* **1998**, *17*, 3070−3076.

(31) Massey, A. G.; Park, A. J. *J. Organomet. Chem.* **1964**, *2*, 245−250.

(32) (a) Chisholm, M. H.; Navarro-Llobet, D. *Macromolecules* **2002**, *35*, 2389−2392. (b) Schilling, F. C.; Tonelli, A. E. *Macromolecules* **1986**, *19*, 1337−1343.

(33) Sheldrick, G. M. *SHELXTL*, Version 5; Siemens: Madison, MI, 1996.

(34) Bradley, D. C.; Harding, I. S.; Keefe, A. D.; Motevalli, M.; Zheng, D. H. *J. Chem. Soc., Dalton Trans.* **1996**, 3931−3936.

(35) For a review, see: Smith, J. G. *Synthesis* **1984**, *8*, 629−656.

(36) (a) Bergquist, C.; Bridgewater, B. M.; Harlan, C. J.; Norton, J. R.; Friesner, R. A.; Parkin, G. *J. Am. Chem. Soc.* **2000**, *122*, 10581−10590. (b) Siedle, A. R.; Lamanna, W. M. U.S. Patent. 5,296,433, 1994. (c) Siedle, A. R.; Lamanna, W. M.; Newmark, R. A.; Stevens, J.; Richardson, D. E.; Ryan, M. *Makromol. Chem. Macromol. Symp.* **1993**, *66*, 215−224.

(37) Chakraborty, D.; Chen, E. Y.-X. *Organometallics* **2003**, *22*, 207−210.

(38) Doerrer, L. H.; Green, M. L. H. *J. Chem. Soc., Dalton Trans.* **1999**, 4325−4329.

(39) Danopoulos, A. A.; Galsworthy, J. R.; Green, M. L. H.; Cafferkey, S.; Doerrer, L. H.; Hursthouse, M. B. *Chem. Commun.* **1998**, 2529−2530.

(40) Jeffrey, G. A. *An Introduction to Hydrogen Bonding*; Oxford University Press: Oxford, U.K., 1997; p 12.

MA034050A